Enantiodifferentiation in Rogers' BOC-D-Val Chiral Stationary Phase

Kenny B. Lipkowitz,* Shawn Antell, and Brian Baker

Department of Chemistry, Indiana University–Purdue University at Indianapolis, Indianapolis, Indiana 46205

Received May 15, 1989

The enantioselective binding of (±)-2,2,2-trifluoro-1-(9-anthryl)ethanol to a BOC-D-Val chiral stationary phase has been successfully simulated. Information from the simulation not amenable to experimentation is extracted and discussed. It is found that both optical isomers bind in the same general region around the chiral stationary phase, but the intermolecular potential energy surfaces for the weakly bound diastereomeric complexes that form upon adsorption are extraordinarily flat. The BOC group is found not to be most responsible for chiral recognition, but it does play a key role in analyte binding. The amide group along with the spacer chain on the chiral stationary phase is found to be most responsible for chiral recognition. The solvent accessible surface area of the BOC-D-Val chiral phase indicates ~75% of the surface to be nonpolar. The polar atoms in this chiral stationary phase tend to reside under an umbrella of hydrocarbon, explaining why the chromatographic separability factor, α, is insensitive to solvent polarity.

Introduction

There now exist a large number of commercially available chiral stationary phases (CSP).[1] An even larger number of noncommercial CSPs have been reported in the literature.[2] These chromatographic stationary phases make it possible to directly resolve racemic mixtures on analytical and preparative scales. In spite of the vast literature on these chromatographic systems, relatively little is known about how these CSPs work.

How do chiral stationary phases recognize and selectively bind one of two mirror image isomers? To address this and to provide insights about chiral recognition not amenable to experimentation we have developed computational tools that allow us to simulate the enantioselective binding process. In this paper we consider the binding of a chiral alcohol to a chiral stationary phase derived from an amino acid. We ask the following questions: Where around the CSP does the analyte bind? Does one enantiomer bind to one part of the CSP while the other enantiomer binds elsewhere, or, do they both bind at the same site? What is the "binding site"? Exactly what atoms are being considered to define a binding site? What portion of the CSP is responsible for enantiorecognition? While the forces between molecules have been exhaustively studied and are thoroughly documented, how these forces work *in concert* to induce selective binding is not yet known. Here we begin addressing these questions and examine how chiral recognition takes place.

System Modeled

In 1987, Rogers' group published a paper on the synthesis and characterization of chiral stationary phases from amino acids and small peptides for liquid chromatography.[3] A large number of CSPs containing a single optically active amino acid or a dipeptide were constructed and tested for their ability to resolve 2,2,2-trifluoro-1-(9-anthryl)ethanol, TFAE, **1**. The best of these CSPs, with the exception of a tripeptide, was found to be the BOC-D-Val CSP appended to silica via an *n*-butyl spacer. In a previous paper we examined the binding of TFAE to the (*R*)-phenylglycine Pirkle phase and refuted the accepted chiral recognition model.[4] In this study we model the binding of **1** to **2**, a truncated analogue of the aforementioned BOC-D-Val CSP.

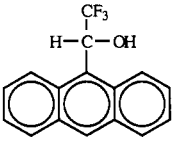

1

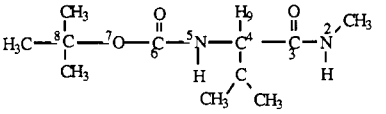

2

As analyte **1** traverses through the column it encounters CSP **2** and forms short-lived diastereomeric complexes held together by weak forces. The following equilibria exist throughout the column:

$$1^R + 2^R \rightleftharpoons 1^R{\cdot}2^R \quad (1)$$

$$1^S + 2^R \rightleftharpoons 1^S{\cdot}2^R \quad (2)$$

Here **1** and **2** refer to analyte **1** and CSP **2**, respectively, and the superscripts *R* and *S* are the Cahn–Ingold–Prelog stereochemical descriptors. Each equilibrium is associated with a free energy of binding, ΔG. These free energies contain the information needed to predict the elution order of **1**; the optical antipode which is more tightly bound to the CSP has a more negative ΔG and will be longer retained on the BOC-D-Val column.

One need not, however, assess ΔG for each equilibrium. Rather, we need only to compute G for the $1^R{\cdot}2^R$ complex and compare it directly with G of the $1^S{\cdot}2^R$ complex. This direct comparison is possible because the left-hand sides of both equilbria are chemically identical. The CSP is the same in both equilibria, and the free energy of the *R* form

(1) Four books on the topic of chiral chromatography have recently been published: (a) Souter, R. W. *Chromatographic Separations of Stereoisomers*; CRC Press: Boca Raton, FL, 1985. (b) *Chromatographic Chiral Separations*, Chromatographic Science Series Vol. 40; Zief, M., Crane, L., Eds.; M. Dekker, Inc.: New York, 1987. (c) Konig, W. A. *The Practice of Enantiomer Separation by Capillary Gas Chromatography*; Huethig Publishing: Heidelberg, 1987. (d) Allenmark, S. G. *Chromatographic Enantioseparation. Methods and Application*; Ellis Horwood Series in Advanced Analytical Chemistry; Chalmers, R. A., Mason, M., Eds.; Ellis Horwood Ltd.: Chichester, 1988.

(2) Recent reviews that describe these phases include: (a) Ward, T. J.; Armstrong, D. W. *J. Liq. Chromatogr.* **1986**, *9*(2,3), 407. (b) Lindner, W.; Pettersson, C. In *LC in Pharmaceutical development*; Wainer, I., Ed.; Aster Publishing; Springfield, 1985; pp 63–131. (c) Shibata, T.; Okamoto, I.; Ishii, J. *J. Liq. Chromatogr.* **1986**, *9*, 313. (d) Wainer, I. *Chromatography Forum* **1986**, 55. (e) Schurig, S. *Kontakte (Darmstadt)* **1986**, *1*, 3. (f) Armstrong, D. W. *Anal. Chem.* **1987**, *59*(2), 84A. (g) Johns, D. *American Laboratory* **1987**, 72. (h) Okamoto, Y. *Chemtech* **1987**, 176. (i) Pettersson, C.; Westerlund, D. *Sven. Farm. Tidskr.* **1987**, *91*(5), 7. (j) Ichida, A. *American Laboratory* **1988**, 100. (k) Hermansson, J.; Schill, G. *Chromatogr. Sci.* (Chromatogr. Chiral Sep.) **1988**, *40*, 245–81. (l) Zief, M. *Chromatogr. Sci.* (Chromatogr. Chiral Sep.) **1988**, *40*, 337–53. (m) Konig, W. A. In *Drug Stereochemistry. Analytical Methods and Pharmacology*; Wainer, I. W., Drayer, D. E., Eds.; Marcel Dekker Inc.: New York, 1988; Chapter 5. (n) Wainer, I. W. *ibid.* Chapter 6.

(3) Hsu, T.-B.; Shah, P. A.; Rogers, L. B. *J. Chromatogr.* **1987**, *391*, 145–60.

(4) Lipkowitz, K. B.; Demeter, D. A.; Parish, C. A.; Darden, T. *Anal. Chem.* **1987**, *59*, 1731–33.

0022-3263/89/1954-5449$01.50/0

of the unbound analyte is the same as the free energy of the *S* form. This is ensured by their enantiomeric relationship. The modeling we present here, consequently, is on the competing diastereomeric complexes on the right-hand side in eq 1 and 2.

Several other points need to be highlighted concerning assumptions we made in this study. First we have assumed a 1:1 complex between CSP and analyte. There may actually exist inhomogeneities on the silica where several CSP molecules are clustered together, but the light loadings by Rogers suggests this is improbable. Second, we neglect the effects of the butyl spacer and of the silica surface. We do this in part because we believe the differential binding of *R* vs *S* analyte to the spacer and to the silica surface is small but also because are uncertain about how to model the amorphous silica gel surface. Finally, we neglect explicit treatment of solvation, again assuming differential solvation is small. Although changes in mobile-phase polarity should result in changes in separability, none is observed experimentally. We will explain why this is so in the discussion. Hence, we model the inherent binding of *R*- and *S*-1 to CSP analogue **2** as a 1:1 complex in vacuo.

Computational Methods

In an earlier paper we described a computational protocol for determining the free energies of weakly bound diasteromeric complexes.[5] The free energy of each diastereomeric complex is approximated as $\bar{E}$, the column averaged interaction energy. The definitions and theoretical underpinning for determining $\bar{E}$ has been published.[5] Here we point out that the free energy depends on the shape of the chiral stationary phase, CSP, the shape of the analyte, A, and the orientation of the two molecules relative to one another. The calculation of $\bar{E}$ reflects our concern that many CSPs are flexible organic molecules that can adopt multiple conformations, each of which can interact with passing analyte in a unique way. It also accounts for the conformational flexibility of the analyte. Our method, then, accounts for the probability that the CSP is in a particular conformation, the probability that the analyte is in a particular conformation as well as the probability that the two molecules are oriented in a particular way in the complex. Because of the enantiomeric relationship between analytes, then, $\Delta\bar{E} = -RT \ln \alpha$, where α is the separability factor which is the ratio of retention times for *R*-1 vs *S*-1.

The quantity we compute, α, is an averaged value corresponding to measurements over a long time period (minutes). The microstates used to determine $\bar{E}$ are obtained by sampling configurations as the analyte is rolled over the van der Waals surface of the CSP. Typically 10^5–10^6 configurations are sampled for the *RR* complex and an equal number for the *RS* complex. The energy of each microstate is computed with a suitable empirical force field. The MM2 force field with bond moments changed to atom-centered charges was used as explained earlier.[6]

The position of the analyte with respect to the CSP is given in polar coordinates (Figure 1). The value of *r* is allowed to vary as we move through θ and ϕ. At each latitude, θ, and longitude, ϕ, a large number of Euler angles are considered. The key point to be made here is that sampling of configurations for the statistical analysis is the same for both *R* and *S* analytes. The definitions of origins,

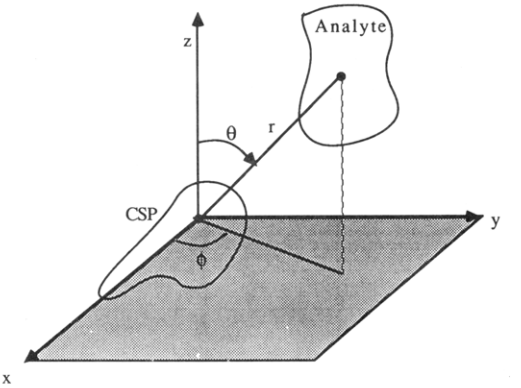

Figure 1. The position of analyte with respect to the chiral stationary phase is given in spherical coordinates (r, θ, ϕ). The origin of the CSP and of the analyte are the stereogenic centers. The alignment of the x, y, and z axes on the CSP is described in the text.

the number of samples taken, and the prescribed tumbling motions for both analytes are precisely the same. This way direct comparisons can be made between binding forces of analytes and we can reconstruct these two otherwise identical experiences to look for differences that we refer to as enantiodifferentiation.

The structures used for the simulations are the same ones used by Still and Rogers who recently published a computational study of the binding of **1** with **2**.[7] The difference between our work and that of Still and Rogers' is that we used rigid body docking and we have replaced the MM2 bond moments with raw atomic charges derived quantum mechanically. The quantum mechanical charges were computed with the AM1 hamiltonian in Stewart's MOPAC program[8] using atomic coordinates obtained from MM2 optimized geometries of **1** and **2**. Another difference between Rogers' work and ours is that we sample a larger number of configurations for the statistical mechanics and we use more than the most stable structure for the CSP. It is our opinion that higher energy conformers of the CSP could play an important role in chiral recognition.

The reader should be aware that computing intermolecular energies with rigid bodies is, in our experience, adequate but not rigorous. It is desirable to account for an "induced fit" as analyte binds to CSP by fully relaxing all internal torsional degrees of freedom during the sampling process. Until recently this was not computationally feasible. We have, nonetheless, been successful with our rigid body approach for two reasons. First we are dealing with diasteromeric complexes that are very weakly bound. Within the weak binding domain one does not expect gross structural changes of either CSP or analyte once complexed (for tight binding we expect our approach to completely fail). Second, we are comparing mirror image isomers using identical sampling procedures so that errors in the computational method tend to cancel. Overall, the method of Rogers and Still allows for induced fit but uses too few configurations for a meaningful statistical mechanical analysis while we sample an adequate number of configurations but do not account for induced fits. As computing machinery becomes faster we will be able to do a rigorous statistical mechanics analysis that accounts for structural changes upon binding.

In the calculations performed here the origin in Figure 1 is the stereogenic center, C4, on CSP **2**. The bond C_4–N_5 is along the x axis and the bond C_4–H_9 is along the y axis.

(5) Lipkowitz, K. B.; Demeter, D. A.; Zegarra, R.; Larter, R.; Darden, T. *J. Am. Chem. Soc.* **1988**, *110*, 3446.
(6) Lipkowitz, K. B.; Baker, B.; Zegarra, R. *J. Comput. Chem.* **1989**, *10*(5), 718–32.
(7) Still, M. G.; Rogers, L. B. *Talanta* **1989**, *36*(1-2), 35–48.
(8) Stewart, J. J. P. *QCPE Bull.* **1983**, *3*(2), 455.

The origin selected on the analyte is the stereogenic carbon. The dielectric constant between the two molecules was set equal to 1.50. Computation of $\bar{E}$ and α assumed temperature T = 298.15 K.

Results and Discussion

In this paper we have sampled a large number of configurations that the system will visit over an infinite time period and used these configurations, in a statistically averaged way, to calculate an averaged value $\bar{E}$. $\bar{E}$ is a macroscopic free energy of interaction between analyte and chiral stationary phase. For the *RR* diastereomeric complex we sample 7.2×10^5 configurations and compute $\bar{E}$ as −5.75 kcal mol^{-1} at 298 K. For the *RS* complex we find $\bar{E}$ to be −5.51 kcal mol^{-1}.

This indicates that the enantiomer with the *R* configuration is more tightly bound to the CSP and will have a longer retention time on the column than does the *S* enantiomer. These results are consonant with experiment.[3] The difference in free energy between these complexes allows us to determine α, the separability factor, by $\Delta\bar{E} = -RT \ln \alpha$. We calculate α = 1.4 and the experimental value is 1.1. Still and Rogers, like us, overestimated the computed value of α in their modeling study.[7] Their calculations were performed with a dielectric constant set to 4.4 to approximate the 60% hexane/40% methylene chloride solvent. Our dielectric was set to 1.5. Still and Rogers feel that this overestimation of α is expected since MM2 ignores factors which increase the retention times of both enantiomers but do not differentiate them such as residual surface silanols and hydrophobic interactions with unreacted spacer. We do not agree with this. We point out that the effects mentioned by Still and Rogers will affect the residence time of both analytes on the column (measured by the capacity factors k) but should not influence α. Changes in the value of α must originate from differential interactions with the CSP, not those mentioned by Still and Rogers. Our overestimation of α is simply an artifact of setting the dielectric of the medium too low. Higher dielectric constants would modulate the nonbonded interactions, making $\bar{E}$ for the *RR* complex closer in energy to $\bar{E}$ for the *RS* complex (an infinitely high dielectric of course would make the CSP invisible to the analyte making $\bar{E}$ identical for both complexes). Increasing the dielectric constant between CSP and analyte would therefore reduce the computed value of α. Nonetheless, both our results and those of Rogers are especially good considering the assumptions and approximations made in both modeling studies. Overall the results of our simulations are in agreement with experiment, allowing us now to extract information that is difficult or otherwise impossible to obtain by experimentation.

The first question we intend to answer is: where around the CSP does the analyte spend most of its time? It is conceivable that one analyte tends to reside around one portion of the CSP while the other analyte resides elsewhere, e.g. frontside or backside binding. To answer this question we consider the intermolecular potential energy surfaces for the *RR* and the *RS* complexes in Figure 2. These surfaces are plots of the intermolecular energy as a function of θ and ϕ, the longitude and the latitude of the analyte around the CSP, as the molecules just touch. Each point on these $\theta\phi$ surfaces represent the intermolecular energy of the system averaged over various conformations of the CSP, various conformations of the analyte, and various orientations of the analyte with respect to the CSP. Inspection of the *RR* and *RS* intermolecular potential energy surfaces reveal multiple docking regions. Furthermore, it is to be noted that these surfaces are very flat

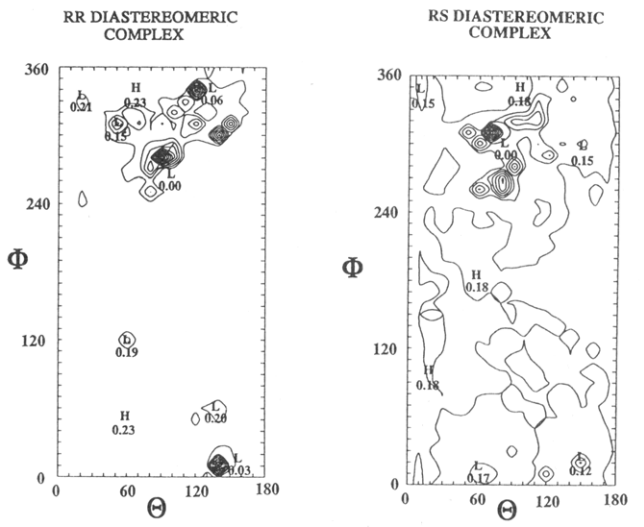

Figure 2. The intermolecular potential energy surfaces (kcal mol^{-1}) for the *RR* and *RS* diastereomeric complexes. The axes refer to latitude, θ, and longitude, ϕ, of analyte 1 around R CSP 2 as defined in Figure 1. Contour lines are spaced every 0.02 kcal. H = high point, L = low point. Global minima are artifically set = zero. Actual data is an equally spaced array of data points 10° apart. Each data point corresponds to a statistically averaged value at that $\theta\phi$ point.

with gently rolling hills, suggesting that the analyte freely slides over broad regions of the CSP. There are no well defined binding regions. For the *RR* complex the global minimum is at ϕ = 280°; θ = 90°. However, another minimum only 0.06 kcal mol^{-1} less stable is found at ϕ = 340°; θ = 120° and yet another minimum which is 0.03 kcal mol^{-1} above the global minimum is located at ϕ = 10°; θ = 140°. For the *RS* surface the global minimum is at ϕ = 320°; θ = 80°. Making comparisons about preferred binding regions from these flat surfaces is not appropriate. All we can say is that broad binding regions between ϕ = 260° and 20° and θ = 40° and 160° are evident on both surfaces suggesting that both *R* and *S* analyte tend to reside in these regions while undergoing wide amplitude sliding or rolling motions with respect to the CSP. These findings are different from earlier work of ours on Pirkle phases where docking regions were found to be more well defined.[9] Nonetheless, like Pirkle phases, we find here that both analytes tend to bind to the same regions around the CSP about equally well, informing us that it is not so important as to where analyte binds but how analyte binds.

The second question we address is: which portion of the CSP is responsible for analyte binding and which portion, if different, is responsible for enantiorecognition? To answer these questions we have developed an algorithm that allows us to partition the total binding energy into fragments on the CSP.[6] In molecular mechanics calculations the nonbonded interactions are computed pairwise-additive. This means we determine the attraction of atom 1 on the CSP with atoms 1–33 (lone pair included as pseudoatoms) on analyte, add to this the attraction of atom 2 on CSP with atoms 1–33 on analyte and so on until, avoiding redundancies, we have summed up the interactions of all atoms on the CSP interacting with all atoms on analyte. All we do is define an atom or a collection of atoms as a fragment and keep track of how much of the total intermolecular interaction in attributable to that fragment.

It is unfair and probably inaccurate to describe the nature of a short-lived diastereomeric complex by a single

(9) Lipkowitz, K. B.; Baker, B. *J. Am. Chem. Soc.*, submitted.

Table I. Binding Energies (kcal mol^{-1}) Attributable to Fragments 1–5

fragment number	RR	RS	discrimination factor
1	−1.3577	−1.1291	0.2286
2	−0.6667	−0.6439	0.0228
3	−1.5179	−1.9059	0.3880
4	−0.4861	−0.6069	0.1208
5	−1.6780	−1.1829	0.4879

structure, even if that structure is the global minimum on the multidimensional potential energy surface. The global minimum along with higher energy structures need to be included in our partitioning analysis. Consequently all microstates used to evaluate $\bar{E}$ are used to determine fragment energies. High energy orientations of analyte around the CSP, in other words, need to be weighted less heavily. This way a single strong ineraction like a hydrogen bond may be offset (weighted less) by other destabilizing interactions of the analyte with the remaining fragments of the CSP. In summary, then, the fragment energies, like $\bar{E}$, represent a Boltzmann weighted, macroscopic view of what each portion the CSP "feels" as the analyte binds to it.

How one divides the CSP into fragments is arbitrary. We have divided the CSP into five sections:

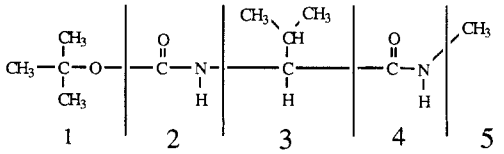

The sum of the binding energies attributable to each fragment adds up to give the total enthalpic component of $\bar{E}$ (we cannot distribute the entropic component which is very small anyway). Table I provides the binding energies attributable to fragments 1–5 for the *R* analyte and for the *S* analyte. The last column in this table is the absolute value of the difference in fragmentation energies between the *RR* and *RS* complexes. This difference is what the CSP "feels" as two mirror image isomers roll over it and is an indication of the magnitude of discrimination each fragment has toward mirror image isomers.

The results of this analysis are enlightening. To begin, we note that the fragment which is least cognizant of differences between *d* and *l* analyte is fragment 2. Why this fragment is least stereodifferentiating is clear from stereoviews (not shown) of the stable conformations of this CSP. We find this amide grouping to be deeply embedded in the interior of the molecule, surrounded by the *tert*-butyl and isopropyl groups. These aliphatic portions of the CSP effectively screen the amide from interacting with the analyte. The fragment most aware of differences between *d* and *l* analyte is fragment 5, the spacer linkage. We hesitate to suggest here that the butyl spacer chain itself is doing most of the chiral recognition because one approximation we made was to truncate the butyl spacer to a simple methyl group, and our results may be an artifact of that approximation. However, we are willing to suggest that fragments 4 and 5 taken together as the amide linkage to the butyl spacer in the real system is playing a major role in enantiodiscrimination. Interestingly, Still and Rogers found in their computational studies that the size of the spacer chain affected the outcome of their results. In future studies we will determine what role, if any, the spacer chains play in chiral separations.

Another way of partitioning the binding energy is to divide the CSP into two fragments. One fragment, hereafter called fragment 1′, corresponds to all the "polar" atoms and the second fragment called fragment 2′ are all of the aliphatic atoms. Table II lists the binding energies attributable to the polar and nonpolar parts of the CSP.

Table II. Binding Energies (kcal mol^{-1}) Attributable to Fragments 1′ and 2′

fragment number	RR	RS	discrimination factor
1′	−1.5803	−1.2781	0.3022
2′	−4.1189	−4.1906	0.0717

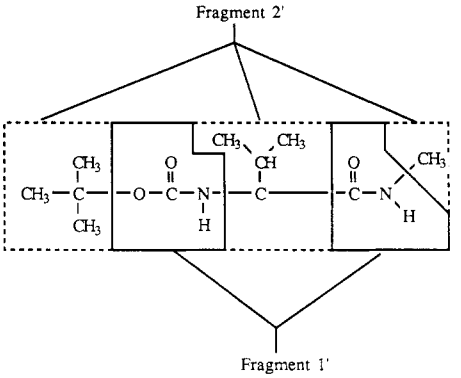

The results of this type of partitioning are also interesting. To begin, we note that most of the binding energy comes from fragment 2′, the aliphatic part of the CSP, rather than from fragment 1′, the polar part. This at first seems counterintuitive, but inspection of stereoviews of the CSP indicated to us that the polar moieties of this CSP are hidden by the nonpolar part of the CSP. To quantitate this we decided to determine the accessible surface area of the CSP. The accessible surface area is the locus of the center of a solvent sphere which is rolled over the van der Waals surface of the solute.[10] Using the Lee and Richards algorithm[11] we find the CSP to have a total surface area of 307 Å^2. The nonpolar saturated surface area is 238 Å^2 while the polar surface area is 69 Å^2. What the solvent sphere sees (as does the analyte) is primarily a nonpolar saturated surface. Indeed approximately $^3/_4$ of the accessible surface of the CSP is hydrocarbon-like in spite of having two amide groups and a butyloxycarbonyl in it!! These results explain why the separability factor, α, is insensitive to mobile-phase solvents. Rogers found that an increase in the percentage of a polar solvent in the eluent decreased the capacity factor, *k*, but kept α essentially constant.[3] For the BOC-D-Val phase using 1% 2-propanol in hexane they found α = 1.10. For the same CSP using 20% methylene chloride in hexane they found α = 1.11. It seems that polar solvents have little effect on this CSP's ability to enantiodiscriminate because the polar solvent can not effectively solvate the polar regions of the CSP since these regions are hidden under an umbrella of hydrocarbon.

Summary

We have successfully simulated the binding of (±)-**1** to BOC-D-Val, **2**. We find the *R* analyte to be longer retained on the *R* CSP in agreement with experiment. Although we are not computing actual retention times as reflected in capacity factors, *k′*, we can compute the relative free energies of binding which may be compared with the separability factor α. From our statistical mechanical modeling we find the *R* analyte to be more tightly complexed with **2** than its mirror image. This suggests the *R*

(10) Richards, F. M. *Methods Enzymol.* **1985**, *115*, 440–464.
(11) Lee, B.; Richards, F. M. *J. Mol. Biol.* **1971**, *55*, 379–400.

enantiomer will be longer retained on the column than the S antipode, which is in agreement with experiment. We overestimate the magnitude of the computed separability factor by underestimating the dielectric of the medium but find the agreement between theory and experiment satisfactory. Information extracted from our simulations that are not amenable to experimentation include the following. (1) There are no well-defined binding sites on this CSP in contrast to earlier studies on Pirkle phases. The intermolecular PESs are extremely flat, allowing 1 to freely slide up and down 2. The reason for this slippery behavior is now clear: the CSP looks more like a ball of hydrocarbon than anything else. (2) Binding originates primarily from hydrophobic portions on the CSP with the analyte. Fully $^3/_4$ of the CSP's accessible surface area is nonpolar in nature. (3) The fragment most cognizant of differences between the chirality of analyte molecules is the amide attached to the spacer chain. We conclude that this part of the CSP is most responsible for enantiodifferentiation while the *tert*-butyl and isopropyl groups are most responsible for analyte binding.

Acknowledgment. This work was funded by the donors of the Petroleum Research Fund, administered by the American Chemical Society, and in part from a grant by the National Science Foundation (Grant CHE-8901828). A grant by Eli Lilly and Company to support Shawn Antell is greatly appreciated. All software developed for this study is made available free of charge by contacting the senior author.

Registry No. (±)-1, 60686-64-8; (*R*)-1, 53531-34-3; (*S*)-1, 60646-30-2; 2, 122902-99-2.

Chemistry of Novel Compounds with Multifunctional Carbon Structure. 5.[1] Molecular Design of Versatile Building Blocks for Aliphatic Monofluoro Molecules by Manipulation of Multifunctional Carbon Structures

Yoshio Takeuchi,* Kazuhiro Nagata, and Toru Koizumi

Faculty of Pharmaceutical Sciences, Toyama Medical & Pharmaceutical University, Sugitani 2630, Toyama 930-01, Japan

Received March 10, 1989

Three kinds of doubly functionalized monofluoromethylene fragments, 1-fluoro-1-nitro-1-(phenylsulfonyl)alkanes (10), 2-fluoro-2-(phenylsulfonyl)alkanoic esters (11), and 2-fluoro-2-nitroalkanoic esters (12), potentially versatile building blocks for the general synthesis of various aliphatic monofluoro molecules, were prepared from the corresponding difunctional compounds 1–3 by monoalkylations (R) and selective fluorinations. The interconversion or reductive removal of each functional group in 10–12 followed by the introduction of the second alkyl groups (R′) at the fluorine-bearing carbon atom was examined. Compounds 12 proved to be useful and practical building blocks for conversions to the various monofluoroalkanes 20–26.

Introduction

The synthesis of aliphatic organofluorine compounds, in contrast to aromatics, has been severely limited. The recent increasing interest in aliphatic fluorine compounds for new materials,[2] biological activity,[3] and mechanistic chemistry[4] led us to attempt to develop general synthetic methods for the preparation of structurally complex fluoroaliphatic compounds. Monofluoro molecules are extremely difficult to prepare because of the inherent problem of stereoselectivity and the high C–F bond reactivity.[5] Although some building blocks for monofluoro compounds have been developed,[6] only simple structures can be derived from them since only a small number of fluorinated starting materials are available.

Scheme I

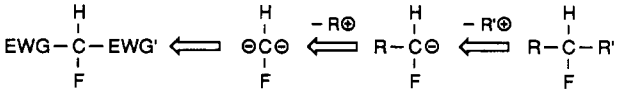

With this situation in mind, we hoped to develop general synthetic pathways to a wide variety of deliberately designed secondary alkyl fluorides by the use of novel monofluoro building blocks that have multifunctionalized carbon structures.[7,8] The development of synthetic approaches and the investigation of the chemical behavior of such geminally functionalized fluorine compounds were also matters of our interest, since these compounds have been so far not investigated. This paper provides a full account of the molecular design of the building blocks and the interconversion of each functional group on the position α to the fluorine.[9]

(1) For Part 4, see: Takeuchi, Y.; Ogura, H.; Ishii, Y.; Koizumi, T. *J. Chem. Soc., Perkin Trans. 1*, in press.

(2) (a) Banks, R. E. *Preparation, Properties, and Industrial Applications of Organofluorine Compounds*; Ellis Horwood Ltd.: Chichester, 1982. (b) Satokawa, T. *Functional Fluorine-Containing Polymers*; Daily Industrial News Ltd.: Tokyo, 1986.

(3) (a) Filler, R.; Kobayashi, Y. *Biomedical Aspects of Fluorine Chemistry*; Kodansha Ltd.: Tokyo, 1982. (b) Filler, R. *Biochemistry Involving Carbon-Fluorine Bonds*; American Chemical Society: Washington, DC, 1976. (c) Welch, J. T. *Tetrahedron* **1987**, *43*, 3123.

(4) For recent examples, see: (a) Cox, D. G.; Gurusamy, N.; Burton, D. J. *J. Am. Chem. Soc.* **1985**, *107*, 2811. (b) Cox, D. G.; Burton, D. J. *J. Org. Chem.* **1988**, *53*, 366. (c) Bordwell, F. G.; Branca, J. C.; Bares, J. E.; Filler, R. *Ibid.* **1988**, *53*, 780. (d) Filler, R.; Cantrell, G. L.; Choe, E. W. *Ibid.* **1987**, *52*, 511. (e) Dolbier, W. R., Jr.; Burkholder, C. R.; Wicks, G. E.; Palenik, G. J.; Gawron, M. *J. Am. Chem. Soc.* **1985**, *107*, 7183. (f) Kitazume, T.; Kobayashi, T.; Yamamoto, T.; Yamazaki, T. *J. Org. Chem.* **1987**, *52*, 3218. (g) Welch, J. T.; Seper, K. W. *Ibid.* **1988**, *53*, 2991. (h) Welch, J. T.; Eswarakrishnan, S. *Ibid.* **1985**, *50*, 5909. (i) Welch, J. T.; Samartino, J. S. *Ibid.* **1985**, *50*, 3663, and references cited therein.

(5) Takeuchi, Y.; Asahina, M.; Hori, K.; Koizumi, T. *J. Chem. Soc., Perkin Trans. 1* **1988**, 1149.

(6) For a recent review, see: Takeuchi, Y. *Synth. Org. Chem., Jpn.* **1988**, *46*, 145.

(7) Takeuchi, Y.; Asahina, M.; Murayama, A.; Hori, K.; Koizumi, T. *J. Org. Chem.* **1986**, *51*, 955.

(8) Takeuchi, Y.; Asahina, M.; Nagata, K.; Koizumi, T. *J. Chem. Soc., Perkin Trans. 1* **1987**, 2203.

(9) Takeuchi, Y.; Nagata, K.; Koizumi, T. *J. Org. Chem.* **1987**, *52*, 5061.

0022-3263/89/1954-5453$01.50/0